EPJ Web of Conferences **94**, 02015 (2015)
DOI: 10.1051/epjconf/20159402015

Strength and failure of a damaged material

Ellen K. Cerreta[1,a], George T. Gray III[1], Carl P. Trujillo[1], Mark L. Potocki[2], Shraddha Vachhani[1], Daniel T. Martinez[1], and Manual L. Lovato[1]

[1]MST-8, Los Alamos National Laboratory, Los Alamos 87545, New Mexico
[2]XTD-PRI, Los Alamos National Laboratory, Los Alamos 87545, New Mexico

Abstract. Under complex, dynamic loading conditions, damage can occur within a material. Should this damage not lead to catastrophic failure, the material can continue to sustain further loading. However, little is understood about how to represent the mechanical response of a material that has experienced dynamic loading leading to incipient damage. Here, this effect is examined in copper. Copper is shock loaded to impart an incipient state of damage to the material. Thereafter compression and tensile specimens were sectioned from the dynamically damaged specimen to quantify the subsequent properties of the material in the region of intense incipient damage and in regions far from the damage. It is observed that enhanced yield stresses result from the damaged material even over material, which has simply been shock loaded and not damaged. These results are rationalized in terms of stored plastic work due to the damage process.

1. Introduction

There are a number of applications that expose structural materials to the extreme environment of dynamic loading. These applications range from aerospace, automotive, civil, and even manufacturing needs. Often times under dynamic loading conditions, which typically impart high stresses (multiple GPa) at high rates, failure of these structural materials can be catastrophic [1,2]. This is even true for ductile, structural metals. For this reason, it is desirable to not only predict the catastrophic failure of these materials but also move toward developing such a robust understanding that will enable next generation materials to be designed to mitigate failure.

Currently, many predictive failure models do not accurately represent failure under dynamic loading conditions [3–5]. This is, in part, attributed to a lack of understanding about the developing microstructure under dynamic loading. One aspect of this microstructure that is of particular importance is the strength of the dynamically loaded or shocked microstructure prior to failure.

For a number of years, multiple investigations have examined the influence of shock loading on the subsequent properties of a material [6–8]. These studies have focused primarily on examining the quasi-static, uni-axial stress response of a metal that had been loaded to peak shock stresses in excess of 5 GPa and then soft recovered for post mortem examination. It has been shown, for high purity metals, that the way in which a material stores defects, determines the role of shock loading. For example, FCC metals that tend to deform through dislocation glide and cross slip, can exhibit enhanced hardening after shock loading [9]. Prestraining FCC metal, by shock loading has been shown to develop a dislocation cell structure and debris within the microstructure. This reduces available glide distances within the material upon any subsequent reloading and thus leads to an observed hardening response over as-annealed material. BCC metals that tend to deform through planar slip, like Ta, display little enhanced hardening after shock loading [10]. Due to the high Peierls stresses inherent in many BCC metals, like Ta and Nb, shock prestraining stores arrays of planar dislocations. These arrays do not substantially work harden the material and therefor do not lead to an enhanced hardening response.

While significant work has been performed to investigate the role of shock loading on subsequent properties of a metal, much less is understood about the role of shock-induced damage on subsequent properties of a material [11]. Specifically, the strength of an incipiently spalled material has received less attention. To this end, here a study is presented that is aimed at understanding the quasi-static, uni-axial stress-strain response of incipiently spalled, high purity, copper. Copper has been selected for this study as its dynamic response and corresponding microstructural evolution have been well characterized, previously.

2. Anisotropic loaded damage and failure models

Simple, maximum, tensile failure criteria through the Johnson-Cook failure models are isotropic, treating all components of the stress tensor equally. The result of failure by these models is the material within a computational element becomes effectively a gas that can not resist further tension. However, when materials fail, due to anisotropic loading, the failure has a directional component although the material may be modified in the directions perpendicular to the failure. By incorporating directional failure in 2D codes, a more 3D material behaviour is achieved. That is by incorporating anisotropic failure models into 2D codes, out-of-plane loads such

[a] Corresponding author: ecerreta@lanl.gov

as hoop stress can be computed correctly, and failure of material within a zone does not result in the material becoming a fluid, but only having failed in directions that exceed failure criteria and the element remains able to resist loads in non-failed directions.

For most materials a non-linear material behaviour model may be adopted with two distinct material mechanical processes: plasticity and damage mechanics. These two processes are influenced by microcrack, microcavity nucleation and coalescence, inclusions, grain boundaries and other discontinuities. With anisotropic loading, the development of degradation becomes complex, and frequently is based on anisotropic damage evolution. The Cauchy stress tensor $\underline{\underline{\sigma}}$ is for a material consisting of metal matrix and voids. This composite is related to the matrix stress through the operation of the damage effect tensor **M:**

$$\underline{\underline{\sigma}} = \boldsymbol{M} : \underline{\underline{\tilde{\sigma}}} \tag{1}$$

where the overscore tilde designates a pure material variable defined over the same area or volume as the analogue composite variable, tensor order is denoted by the number of underbars and bolded symbols are fourth-order tensors. The simplest selection for $\boldsymbol{M}$ is the isotropic damage form:

$$\boldsymbol{M} = (1 - D)\,\boldsymbol{\delta} \tag{2}$$

where D is the amount of isotropic damage, assumed to be the porosity (a ratio of the void volume to the current volume ignoring elastic volume changes) and $\boldsymbol{\delta}$ is the fourth order identity tensor ($\boldsymbol{\delta}_{ijkl} = \boldsymbol{\delta}_{ij}\ \boldsymbol{\delta}_{kl}, \boldsymbol{\delta}_{ij}$ designating the Kronecker delta function).

To obtain failure directions, the material is first rotated by polar decomposition to the material frame with principal stress directions. For maximum stress failure to occur the n_1 component of the traction in the n_1 direction $t_1 = \sigma \cdot n_1$ reaches a certain failure strength τ_1:

$$\sigma^* = \sigma - (n_1 \cdot \sigma \cdot n_1)\, n_1 \otimes n_1 \tag{3}$$

where n_1 is the normal to the failure surface in material coordinates. When:

$$t_1 \cdot n_1 = (n_1 \cdot \sigma \cdot n_1) \geq \tau_1 \tag{4}$$

the modified stress tensor satisfies

$$\left(n_1 \cdot \sigma^* \cdot n_1\right) \geq 0. \tag{5}$$

Damage evolution often accompanies the relaxation of stress in the direction of failure, due the formation of damage. The modified tensor σ^* is symmetric, but the trace is no longer pressure. To calculate plastic deformation, new traceless deviators are computed:

$$s^* = \sigma^* - \left(\frac{1}{3}\right) Tr\sigma^* I \tag{6}$$

where I is the identity matrix. After a failure in one direction, failure in a second direction occurs when:

$$\sigma^{**} = \sigma^* - (n_1 \cdot \sigma \cdot n_2)\, n_2 \otimes n_2 \tag{7}$$

$$t_1 \cdot n_2 = (n_1 \cdot \sigma \cdot n_2) \geq \tau_2. \tag{8}$$

Figure 1. Optical image of the incipiently damaged, shock loaded Cu specimen.

The values τ_1 and τ_2 are material properties that could be functionals that are updated as the damage effect tensor, and are typically dependent on temperature, strain rate, total strain, initial conditions, and more. These functionals have to be determined by experiment, be non-negative, and are then entered into the model as parameters.

3. Experiments

Oxygen free, high conductivity (OFHC) copper was utilized in the as-annealed condition (600 °C, 1 hour, in vacuum) for all experiments. This as-annealed Cu had a nearly random texture and a 60 μm, equiaxed grain structure. Details about this material, such as processing, chemistry and microstructure, can be found elsewhere [12]. From this as-annealed material, 4 mm in height by 40 mm in diameter right cylinders were sectioned. These cylinders were assembled into a momentum trapping fixture made of a low purity Cu material and schematically described elsewhere [13]. This material was shocked loaded using a plate impact configuration, in a 100 mm gas gun, and soft recovered. The impactor was a 2 mm thick quartz flyer that was launched at 131 m/s. This plate impact velocity and plate material were chosen as they had been previously shown to impart an early stage of incipient damage to copper [12]. This damage was known to be in the form of uncoalesced, small voids, indicative of the early stages of ductile damage.

The soft-recovered specimen was cross-sectioned and prepared using standard metallographic techniques. The final polishing step was performed with a 0.5 μm colloidial silica solution. The specimen was then viewed optically to examine location and extent of the incipient damage within the material. An image of the entire cross section of the specimen is given in Fig. 1.

To further analyse deformation and damage imparted to the Cu specimen, electron back-scattered diffraction (EBSD) was performed. Data was collected from the three, boxed regions labelled in Fig. 1. Data was utilized to generate both inverse pole figure (IPF) as well as kernel average misorientation (KAM) maps to assess meso-scale deformation and stored work in the form of misorientation, respectively. KAM is the average mis-oreintation between a point and its neighbors [14].

Finally, quasi-static, uni-axial test specimens were machined from the soft recovered Cu sample. Tension and compression specimens were machined. Figure 2 shows the locations of each tensile and compression specimen with respect to the primary damage field. Compression specimens were right, regular cylinders that were 2.4 mm in height and 2.6 mm in diameter. Dimensions for the tensile specimens are given in Fig. 3. All specimens were

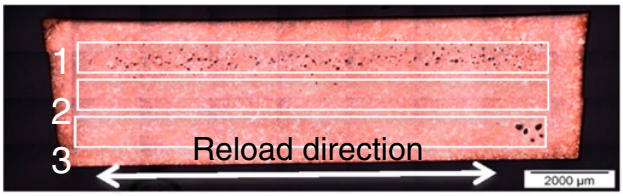

(a)

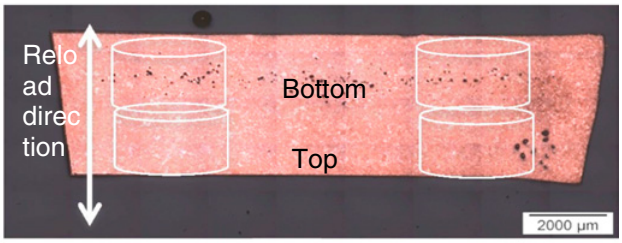

(b)

(c)

Figure 2. Schematics for the location in which (a) tensile and (b) compression specimens were cut, (c) gives a plan view of all specimen types sectioned from the shock loaded sample.

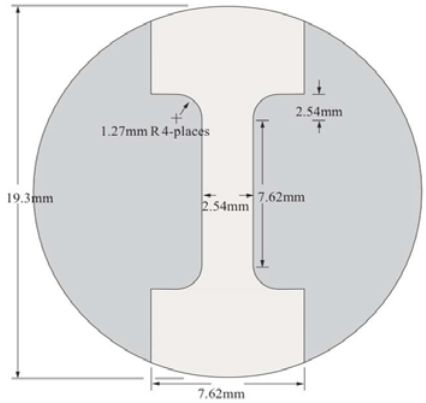

Figure 3. Dimensions for the tensile specimens sectioned from the shock loaded Cu sample.

tested at room temperature and 0.001/s. The three tensile specimens were sectioned from regions 1(most damage) and then 2 and 3 (least damage) as shown in Fig. 2a. Eight compression specimens were sectioned as shown in Figs. 2b and c. Specimens labelled "top" had less damage than specimens labelled bottom.

4. Results

4.1. Microstructure analysis

To quantify the incipient damage imparted to the shock loaded Cu, optical images such as Fig. 1, were used.

Table 1. Damage Statistics for Regions Labelled in Fig. 1.

Region	Avg. size (μm^2)	% Area of void
1	263.6	0.33
2	33.4	0.01
3	19.3	0.02

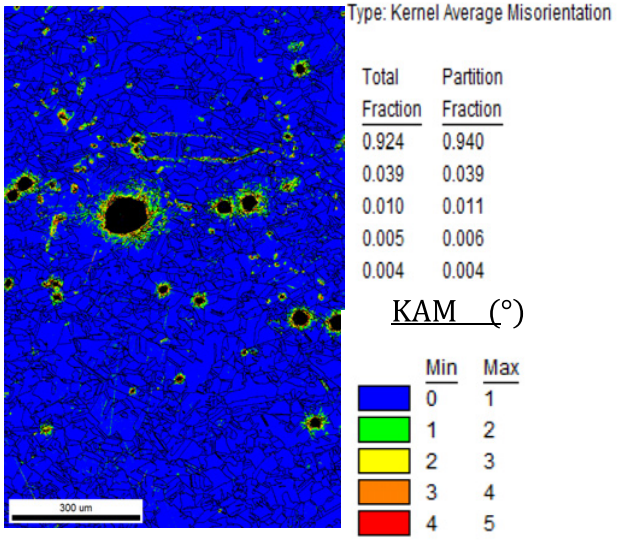

Figure 4. KAM map of region 1 from Fig. 1 showing misoreintation around voids in the incipiently damaged Cu sample.

Images revealed a ductile damage field of uncoalesced voids expected for Cu shocked to the conditions described above. Damage was quantified in terms of void count, total area of voids, average void size, and percent area of void. These data were collected from regions 1–3, given in Fig. 1. J-image software tool was utilized to perform the quantitative analysis of optical images that had been thresholded to black and white contrast. Average void size and percent area of voids data are given in Table 1. Region 1 was observed to have the most damage, with less damage in regions 2 and 3.

After the optical analysis of the damage had been completed, the cross-sectioned Cu specimen was examined via EBSD. Initial analysis revealed that there was little evidence of damage beyond void formation. No shear bands were present. Additionally, KAM maps were generated for regions 1–3. These maps showed little evidence of misoreintation developed during shock loading, except in regions near the voids. An example of one of the KAM maps is given in Fig. 4 for region 1. This was the region that displayed the most significant amount of misorientation as it had the most damage. This is important, because misorientation mapping is a tool for examining stored defects within a microstructure. It would be expected in a dynamically deformed microstructure, that higher degrees of misorientation would correlate with increased density of stored defects, such as dislocations [15, 16].

4.2. Quasi-static mechanical testing

Quasi-static mechanical tests were conducted on the eight compression specimens and three tension specimens

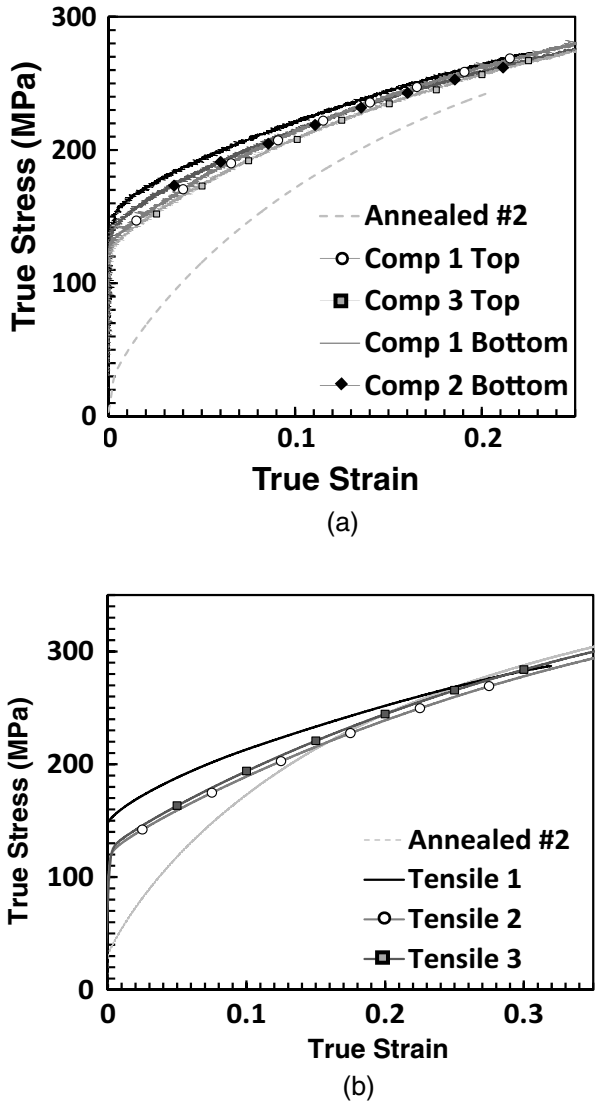

Figure 5. Quasi-static stress-strain data of incipiently damaged Cu: (a) compressive and (b) tensile response.

sectioned from the incipiently damaged Cu sample. For the tension specimens, Tensile 1 corresponds to the tensile specimen sectioned from region 1 shown in Fig. 2a. Tensile 2 and 3 were sectioned from regions 2 and 3, respectively. Compression specimens were tracked with regard to the top and bottom of the shock loaded specimen. For labelling purposes, compression specimens that came from the top of the shock loaded sample were the specimens that contained less incipient damage. The converse was true for compression specimens with a "bottom" designation. The mechanical test data in compression and tension is given in Fig. 5a and b. Only four representative compression tests are shown in Fig. 5a for the sake of clarity. For the purpose of this comparison, tensile and compressive stress-strain responses of as-annealed Cu are also provided.

It can be seen from Fig. 5 that all the quasi-static reload specimens displayed an enhanced hardening response over as-annealed Cu. Interestingly, this is most pronounced in the specimens with the highest volume fraction of incipient damage due to shock loading: "bottom" quasi-static, reload compression specimens and tensile 1. This enhanced hardening is observed upon initial yield. The work hardening response appears to be similar for all of the quasi-static, reload specimens and significantly lower as compared to the work hardening response observed in the as-annealed Cu specimens.

5. Discussion

The quasi-static reload data in tension and compression shows that all of the shock loaded specimens display an enhanced hardening as compared to the as-annealed, high-purity Cu. This indicates that during the shock process, significant work hardening of the Cu sample occurs. This work hardening is directly tied to the isotropic damage term D in Sect. 2 above. This yields material that contains a significant degree of stored plastic work. In turn, this stored work leads to enhanced strength of the material. This response was expected in tensile specimens 2 and 3 and from compression specimens labelled "top". These specimens did not display a high degree of damage imparted to them during the shock loading process, and work by Gray et al. [8,9,17] has already shown that stored work during shock loading leads to enhanced hardening in FCC metals like Cu.

Prior to this study, the response of material that had sustained dynamic damage was less well understood than material that had only been shock loaded but had not experienced the early stages of failure, such as void nucleation and growth [11]. In this case, the behaviour of "bottom" compression specimens and tensile 1 was less predictable. From Fig. 5, it is clear that these specimens, with a modest amount of damage, display enhanced hardening in excess of the shock loaded specimens from other regions in the Cu sample. This is rationalized in terms of the response of the quasi-static reload specimens with relatively less damage and the KAM map, Fig. 4. KAM maps from region 1, showing enhanced misoreintation as compared to regions 2 and 3. This enhanced misoreintation does not exist in the bulk of the shock loaded microstructure, but is measureable around the voids. This is postulated to be caused by the significant slip activity required for void growth. All of the regions experienced significant work hardening due to shock loading and therefore display enhanced hardening as compared to the as-annealed Cu material. In the case of specimens that encompassed material from region 1, that enhanced hardening would be expected to be higher based on the measureable additional plastic work in the form of higher dislocation density around the voids. The small enhancement in hardening observed for tensile 1 and "bottom" compression specimens correlate with the expected contribution to hardening from the small volume of significantly misoriented material around the voids.

The stored work due to shock loading does not only influence yield, but also influences the work hardening response of the Cu material. Here, it is observed to lead to lower work hardening rates than in the as-annealed copper. This lower rate of work hardening can be associated with a less stable dislocation substructure that can promote catastrophic failure [16,18]. It follows that there is a critical amount of stored work in a microstructure after

which the mechanical response of the material is unstable and failure readily results. This is observed in material that has received significant rolling reductions [18]. If shock loaded material behaves similarly, then there should be a critical amount of damage after which enhanced hardening over shock loaded material with no damage and material may not be observed. Future studies will probe the effect of increasing volume fraction of damage on subsequent mechanical properties.

6. Conclusions

This study examined the role of ductile, incipient, dynamic damage imparted during a spallation loading experiment on subsequent mechanical properties of copper. It was found that the mechanical response of Cu is significantly altered due to shock loading. This correlates well with what has been observed previously for shock loaded FCC metals that had not incipiently spalled. Interestingly, material that had experienced a modest degree of dynamic damage displayed an enhanced hardening even in excess of the shock-loaded material without damage. This is attributed to the contribution of the additional stored plastic work contained in the volumes surrounding voids.

Los Alamos National Laboratory is operated by LANS for the NNSA of the US Department of Energy under Contract No. DE-AC52-06NA25396.

References

[1] M. Meyers, Y. Xu, Q. Xue, M. Perez-Prado, T. McNelley. Acta Mater. **51**, (2033).
[2] N. Bourne, *Materials in Mechanical Extremes*. (Cambridge University Press, Canbridge, 2013).
[3] L. Murr, K. Staudhammer, M. Meyers, *Metallurgical Applications of Shock Wave and High Strain Rate Phenomena*. (Marcel Dekker, Inc., New York, 1986).
[4] C. Bronkhorst, B. Hansen, E. Cerreta, J. Bingert. J. Mech. Phys. Sol. **55**, 2351–2383 (2007).
[5] B. Boyce, S. Kramer, H. Fang. Int. J. Fracture **186**, 5–68 (2104).
[6] E. Cerreta, G.T. Gray, R. Hixson, P.A. Rigg, D.W. Brown. Acta Mater. **53**, 1751–1758 (2005).
[7] G.T. Gray. (American Institue of Physics, 1994), pp. 1103–1106.
[8] G.T. Gray. Mat. Res. Symp. Proc. **499**, 87–98 (1998).
[9] G.T. Gray, K. Vecchio. Metal. Mater. Trans. A **26A**, 2555–2563 (0ctober 1995, 1995).
[10] S.R. Chen, G.T. Gray III. Metal. Trans. A **27**, 2994–3006 (1996).
[11] G. Gray, N. Bourne, paper presented at the Dislocations, Plasticity, Damage, and Metal Forming: Material Response and Multiscale Modeling, 2005.
[12] J. Escobedo, D. Dennis-Koller, E. Cerreta, B. Patterson, C. Bronkhorst, B. Hansen, D. Tonks, R. Lebensohn. J. Appl. Phys. **110**, 033513 (2011).
[13] A.K. Zurek, W.R. Thissell, D.L. Tonks, R. Hixson, F. Addessio. J. Phys. IV **7**, 903–908 (1997).
[14] S.I. Wright, M.M. Nowell, D.P. Field. Microscopy and Microanalysis **17**, 316–329 (2011).
[15] J. Bingert, V. Livescu, E. Cerreta, in *Electron Backscatter Diffraction in Materials Science,* A. Schwartz, M. Kumar, B. Adams, D. Filed, Eds. (Springer, New York, 2009), pp. 301–316.
[16] E. Cerreta, J. Bingert, G. Gray, C. Trujillo, M. Lopez, C. Bronkhorst, B. Hansen. Inter. J. Plasticity **40**, 23–38 (2013).
[17] G.T. Gray, N. Bourne, J. Millett. J. Appl. Phys. **94**, 6430–6436 (2003).
[18] H. Fujiwara, T. Sato, A. Kamio. J. Japan Inst. Metals **64**, 641–650 (2000).